Transactions of the Korean Nuclear Society Spring Meeting
Jeju, Korea, May 7-8, 2026

Development of a MATLAB-Based Lumped-Parameter Dynamic Analysis Methodology for Hydraulically-Operated PECCS Valves of i-SMR

Jeong-won Han [a], Young-seok Bang [a], Young-jae Park [a*]
[a]*FNC Technology Co., Ltd., 13 Heungdeok 1-ro, Giheung-gu Yongin-si, Gyeonggi-do, Republic of Korea*
[*]*Corresponding author: ypark1227@fnctech.com*

Keywords : i-SMR, PECCS valves, Dynamic behavior analysis, Lumped-parameter model, MATLAB

1. Introduction

The Innovative Small Modular Reactor (i-SMR) employs a Passive Emergency Core Cooling System (PECCS) that ensures adequate core cooling following a loss-of-coolant accident (LOCA) by supplying coolant from the containment vessel (CV) to the reactor pressure vessel (RV) [1]. The PECCS function is initiated by a set of hydraulically-operated, spring-assisted spool valves that actuate in response to the differential pressure condition between the RV and CV. Accurate prediction of the dynamic behavior of these valves including their opening timing, set pressure accuracy, and potential for oscillatory instability is essential for the design qualification and safety assessment of the PECCS.

Previous work by the authors established a MATLAB-based numerical framework for the coupled pressure-displacement dynamics of the PECCS valves [2] and analyzed spool-retainer collision behavior [3]. While these studies successfully captured the fundamental valve dynamics, the flow force model can be further refined to represent the fluid momentum effects more accurately. Furthermore, the use of a fixed discharge coefficient for all internal orifices may not fully account for the multi-stage geometry of the internal passages. Since the flow force acts exclusively in the valve-closing direction, improving its representation contributes to more accurate pressure predictions. Additionally, a Reynolds-number-dependent treatment of the discharge coefficient is expected to capture the inherent flow resistance characteristics of multi-stage orifice configurations better.

This paper presents two key enhancements to the methodology: (1) a flow force model based on the Reynolds Transport Theorem (RTT) [4, 5] that accounts for the steady-state momentum flux and the transient spool-velocity-induced damping; and (2) a multi-stage orifice equivalent discharge coefficient model that extends existing two-stage orifice analyses [6] to three-stage configurations. Because the dynamic actuation of the spool is governed by the balance between the internal differential pressure and the opposing spring force, accurately predicting the transient chamber pressures is critical. Therefore, this study replaces the fixed discharge coefficient assumption with an improved, Reynolds-number-dependent value that accounts for the multi-staged contraction geometry of the internal passages. The analysis is conducted on a virtual valve model with a hydraulic architecture analogous to the PECCS valves.

2. Modeling Methodology

2.1 Valve Configuration

The system consists of a main valve (MV) and a Spurious Opening Protection Module (SOPM), as shown schematically in Figure 1. The SOPM prevents inadvertent opening of the MV under unintended pressure fluctuations. The internal fluid domain is discretized into multiple control volumes (CVs), each representing a distinct chamber. Adjacent CVs are connected by internal orifices, and the spool-type disks of the MV and SOPM actuate to open and close their respective ports connecting the RV and the CV.

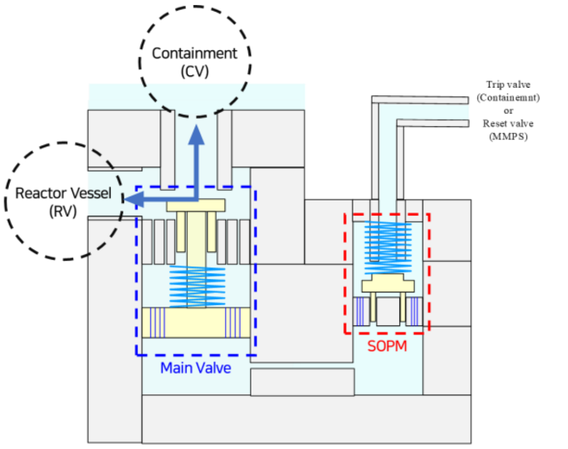

Fig. 1. Schematic of the PECCS Valve System.

2.2 Governing Equations

Using a lumped-parameter approach, each control volume is governed by mass conservation with fluid compressibility. The rate of pressure change in the *i*-th control volume is derived from the continuity equation as follows:

$$\frac{dP_i}{dt} = \frac{\beta}{V_i}\left(\Sigma Q_{in,i} - \Sigma Q_{out,i} - \frac{dV_i}{dt}\right) \tag{1}$$

where β is the fluid bulk modulus, V_i is the *i*-th volume, and dV_i/dt is the volume change rate due to spool displacement. The flow rate through MV and SOPM is modeled by the classical orifice equation:

$$Q = C_d \cdot A(x) \cdot \sqrt{\frac{2|\Delta P|}{\rho}} \cdot \mathrm{sign}(\Delta P) \quad (2)$$

The equations of motion for the MV and SOPM spools are:

$$m_m \ddot{x}_m = F_{p,m} + F_{s,m} + F_{d,m} + F_{flow,m} \quad (3)$$
$$m_b \ddot{x}_b = F_{p,b} + F_{s,b} + F_{d,b} + F_{flow,b} \quad (4)$$

where F_p is the net pressure force, F_s is the spring force, F_d includes viscous damping, and F_{flow} is the flow force.

2.3 Multi-Stage Orifice Modeling

The internal orifices connecting adjacent control volumes in the PECCS valve are long orifices ($L/d \gg 1$) with multiple staged diameter reductions. While the discharge coefficient of single orifices has been extensively studied, the behavior of multi-stage configurations remains less explored. For long orifices, Darcy-Weisbach friction contributes to total pressure loss [5], and when multiple stages are present, the contraction and friction losses interact in a Reynolds-number-dependent manner that cannot be captured by a single constant discharge coefficient (C_d).

Gao and Wu [6] analyzed the two-stage orifice by applying the Bernoulli equation between consecutive flow sections. The total resistance coefficient for the j-th stage, comprising the local contraction loss ξ and the wall friction, is defined as:

$$\Sigma\xi_j = \xi_{j,j+1} + \lambda_j \frac{L_j}{d_{j+1}} \quad (5)$$

where $\xi_{j,j+1}$ is the sudden-contraction loss coefficient at the stage entrance, λ_j is the Darcy friction factor, L_j is the stage length, and d_{j+1} is the stage diameter. They showed that the equivalent discharge coefficient for the two-stage case is:

$$C_{d,\text{two-stage}} = \frac{1}{\sqrt{(1+\Sigma\xi_2) + (1+\Sigma\xi_1)\, m_2^4 - 2m_3^2}} \quad (6)$$

where $m_j = d_{j+1}/d_j$ denotes the diameter ratio of the downstream section to the upstream section (i.e., the (j+1)-th section diameter divided by the j-th section diameter).

In the present work, we extend this approach to a general N-stage orifice. For an orifice with N stages, we label the upstream chamber as section 1, the successive stages as sections 2 through N+1, and the downstream chamber as section N+2. Applying the Bernoulli equation across each stage yields:

$$p_j = p_{j+1} + \left(1 + \Sigma\xi_j\right) \frac{\rho\, u_{j+1}^2}{2}, \quad j = 1, 2, \ldots, N \quad (7)$$

The incompressible continuity equation relates the velocities through the diameter ratios:

$$u_j = m_j^2 \cdot u_{j+1} \quad (8)$$

For the expansion from the last stage into the downstream chamber, the momentum equation gives:

$$p_{out} = p_{N+1} + \rho\, m_{N+1}^2\, u_{N+1}^2 \quad (9)$$

where p_{out} is the downstream chamber pressure and the higher-order term m_{N+1}^4 has been neglected ($m_{N+1} \ll 1$). Substituting Eqs. (7)–(9) and expressing all velocities in terms of the last-stage velocity u_{N+1}, the total pressure drop between the upstream and downstream chambers becomes:

$$\frac{2(p_{in} - p_{out})}{\rho} = \left\{ \sum_{j=1}^{N} \left[(1+\Sigma\xi_j) \prod_{k=j+1}^{N} m_k^4 \right] - 2\, m_{N+1}^2 \right\} u_{N+1}^2 \quad (10)$$

The equivalent discharge coefficient is:

$$C_{d,eq} = \frac{1}{\sqrt{\sum_{j=1}^{N} \left[(1+\Sigma\xi_j) \prod_{k=j+1}^{N} m_k^4 \right] - 2\, m_{N+1}^2}} \quad (11)$$

For the three-stage case (N = 3), Eq. (11) expands to:

$$C_{d,eq} = \frac{1}{\sqrt{(1+\Sigma\xi_1)\, m_2^4 m_3^4 + (1+\Sigma\xi_2)\, m_3^4 + (1+\Sigma\xi_3) - 2m_4^2}} \quad (12)$$

2.4 Flow Force Modeling

The flow force on the spool is derived from the Reynolds Transport Theorem (RTT). The general form of the RTT-based force on a spool valve control volume is [4]:

$$F = \rho L_d \frac{\partial Q}{\partial t} - \rho \frac{Q^2}{A} \cos\theta \quad (13)$$

Substituting the orifice equation $Q = C_d A(x)\sqrt{(2|\Delta P|/\rho)}$ and expanding dQ/dt via the chain rule yields two physically distinct components. The steady-state flow force arises from the change in fluid momentum direction at the metering orifice and always acts in the valve-closing direction:

$$F_{ss} = \sigma \cdot 2 C_d C_v A(x) |\Delta P| \cos\theta \quad (14)$$

where C_v is the velocity coefficient, θ is the jet angle, $A(x)$ is the metering area, and σ is a smooth activation function that transitions the force to zero near valve closure. The transient velocity term arises from spool-motion-induced area change and acts as velocity-proportional damping:

$$F_{tv} = -\sigma \cdot \rho L_d C_d \pi d \sqrt{\frac{2|\Delta P|}{\rho}} \cdot v \qquad (15)$$

The total flow force is $F_{flow} = F_{ss} + F_{tv}$.

3. Results and Discussion

3.1 Analysis Conditions

The valve operability is evaluated using time-dependent RV and CV pressure histories obtained from a postulated LOCA transient analysis. At the onset (t = 0), the RV pressure is 15.5 MPa and the CV pressure is approximately vacuum (0.01 MPa).

All internal control volumes are initially at the RV pressure at $t = 0$. The MV starts fully closed (x_m = 8 mm) and the SOPM fully open (x_b = 0 mm). The ODE system is integrated using MATLAB's ode15s stiff solver with tolerances of 10^{-6}.

3.2 Valve Actuation Sequence

The actuation proceeds in two stages as shown in Fig. 2. As the RV depressurizes (Fig. 3), the trip valve opens at the set point, connecting the SOPM upper chamber to the containment and releasing pressurized fluid. The resulting net downward force closes the SOPM (displacement increases from 0 to 5 *mm*). The SOPM closure isolates the MV internal chambers from the trip line.

With the SOPM closed, continued RV depressurization causes the spring force to exceed the hydraulic pressure force, opening the MV spool (displacement decreases from 8 mm toward 0 mm) and establishing the CV-to-RV flow path.

Figure 3 shows the transient pressure histories of all internal control volumes along with the RV and CV boundary pressures. During the initial hold period, the internal chambers remain in pressure equilibrium with the RV. Upon trip valve actuation, the tube pressure rapidly drops, triggering pressure transients throughout the interconnected chambers. The pressure dynamics during the actuation window exhibit the coupled interaction between spool displacement and chamber pressures, a phenomenon that can only be captured through the lumped-parameter multi-CV approach. After MV opening, all internal pressures converge to approximately 1 MPa, consistent with the eventual RV–CV pressure equilibrium.

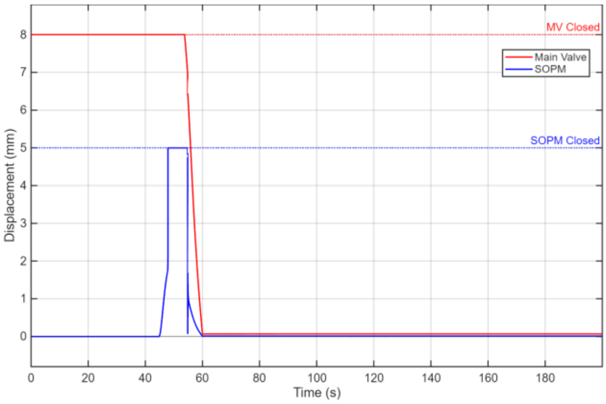

Fig. 2. Spool displacement of MV and SOPM according to time.

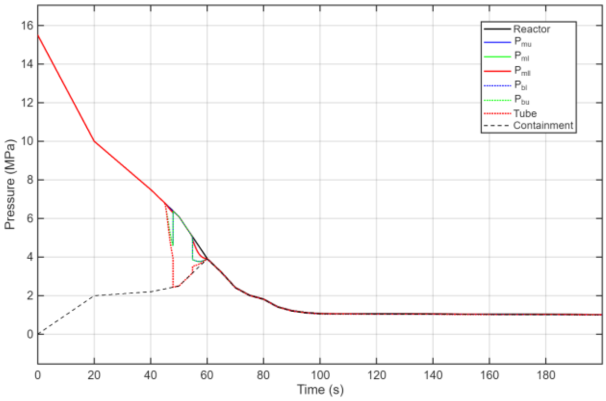

Fig. 3. Transient pressure histories of internal control volumes and boundary conditions.

3.3 Effect of Enhanced Modeling

Figure 4 compares the MV opening transient under four analysis cases: (1) the original model without flow force or multi-stage orifice modeling, (2) with flow force only, (3) with multi-stage orifice only, and (4) the improved model incorporating both enhancements. The original model predicts the fastest opening. The addition of flow force (Case 2) produces a noticeably slower opening transient, as the flow force acts exclusively in the valve-closing direction, providing a momentum-based resistance during the rapid opening phase. The multi-stage orifice model (Case 3) also delays opening by altering the internal pressure dynamics through a Reynolds-number-dependent equivalent discharge coefficient that varies with the flow conditions. The improved model (Case 4) combines both effects, resulting in the most gradual opening transient and demonstrating that these enhancements produce a more physically realistic prediction of the valve dynamics.

Figure 5 presents a comparative force decomposition between the original model (a) and the improved model (b). In the original model, the net force becomes negative after the MV passes through its equilibrium position, driven by the rapid decay of the pressure force while the spring force remains significant. In the improved model, the flow force provides a significant positive (closing-direction) contribution during the opening transient, effectively offsetting the negative pressure force contribution. This restoring-force mechanism maintains the net force near zero in the improved model, preventing the large negative excursion observed in the original model. The physical implication is that the flow force acts as a self-regulating damping mechanism: as the valve opens and flow increases, the momentum-based reaction force resists further opening, providing inherent stability to the actuation process.

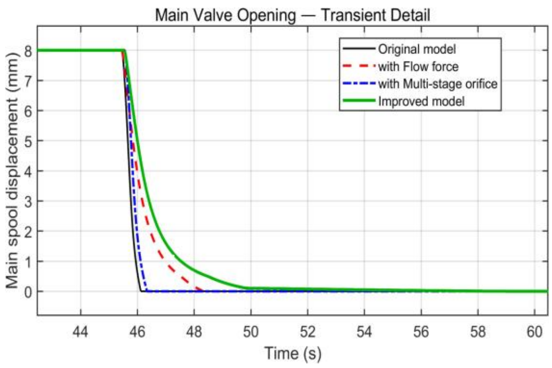

Fig. 4. Comparison of MV opening transient under four analysis cases.

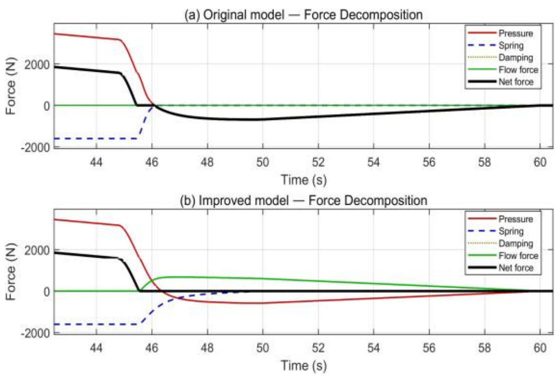

Fig. 5. Force decomposition: (a) Original model vs. (b) Improved model.

4. Conclusions

This paper presented two enhancements to the MATLAB-based lumped-parameter dynamic analysis methodology for PECCS valves: a flow force model based on the Reynolds Transport Theorem and a multi-stage orifice equivalent discharge coefficient model. A four-case comparison was conducted to isolate the individual and combined effects of each enhancement under LOCA boundary conditions representative of the i-SMR PECCS system.

The incorporation of the flow force model yielded a more physically realistic valve response by capturing the closing-direction momentum reaction that is inherently present during spool motion but was previously unaccounted for. Force decomposition analysis confirmed that the flow force serves as a self-regulating damping mechanism, contributing to a more stable actuation transient compared to the original model. In addition, the multi-stage orifice modeling demonstrated that the unique staged-contraction geometry of the internal orifices meaningfully influences the transient pressure dynamics and, consequently, the valve opening characteristics. This confirms that the conventional assumption of a fixed discharge coefficient is insufficient for accurately representing the flow resistance of such complex internal passages. The theoretical extension of the multi-stage orifice model to general *N*-stage configurations provides a generalized analytical framework applicable to various internal orifice designs.

Future work will focus on validation against experimental data and application of the methodology to the actual PECCS valve design for the i-SMR.

ACKNOWLEDGEMENT

This paper was supported by the Innovative Small Modular Reactor Development Agency grant funded by the Korea Government(Ministry of Science and ICT, MSIT) (No. RS-2023-00321928).

REFERENCES

[1] S. G. Lim, H. S. Nam, D. H. Lee, and S. W. Lee, Design Characteristics of Nuclear Steam Supply System and Passive Safety System for Innovative Small Modular Reactor (i-SMR), Nuclear Engineering and Technology, Vol.57, p.103697, 2025.

[2] J. W. Han, Y. J. Park, Y. S. Bang, and Y. C. Choi, Development of Dynamic Behavior Prediction Model for Pilot-Operated Spool Valves, Proceedings of the KSFM Winter Conference, Jeju, Korea, Dec. 3-6, 2025.

[3] Y. S. Bang, Y. J. Park, Y. C. Choi, S. S. Jeon, and S. J. Hong, Analysis of Dynamic Response of Hydraulic Operated Valves of Passive ECCS using MATLAB, Proceedings of the KSFM Winter Conference, Jeju, Korea, Dec. 3-6, 2025.

[4] N. D. Manring and S. Zhang, Pressure Transient Flow Forces for Hydraulic Spool Valves, Journal of Dynamic Systems, Measurement, and Control, Vol.134(3), p.034501, 2012.

[5] H. E. Merritt, Hydraulic Control Systems, John Wiley & Sons, New York, 1967.

[6] H. Gao and J. Wu, Investigation of Flow Through the Two-Stage Orifice, Engineering Applications of Computational Fluid Mechanics, Vol.13(1), pp.117-127, 2019.